



**Acoustics'08
Paris**
June 29-July 4, 2008

www.acoustics08-paris.org

Acoustic waves generated by a laser point pulse in a micrometric fiber

Damien Segur^a, Alexander Shuvalov^a, Yong Dong Pan^b, Nikolay Chigarev^c,
Clément Rossignol^a and Bertrand Audoin^a

^aLMP, UMR CNRS 5469, Université Bordeaux I, 351, cours de la Libération, 33405 Talence,
France

^bInstitute of Acoustics, Tongji University, 200092 Shanghai, China

^cLPEC/UMR 6087/CNRS/Université du Maine, Avenue Olivier Messiaen, 72085 Le Mans
Cedex 09, France

d.segur@lmp.u-bordeaux1.fr

Cylindrical parts are widely used in industry at very different scales from rotating axis of engines to carbon fibers used in composite materials. Consequently, an increasing demand exists for their non destructive evaluation. The laser ultrasonics technique providing a non-contact generation and detection process is suited for the study of acoustic waves in cylindrical structures. In previous works, authors have studied millimetric-sized cylinders. In this paper, we present first result obtained on a tungsten micrometric fiber thanks to a pump-probe femtosecond laser technique. Experiments are compared to a two dimensionnal model for acoustic waves generation and propagation in cylinders taking into account light penetration depth.

1 Introduction

Having emerged in the 80s, the laser ultrasonics technique with its non-contact generation and detection process overpasses the difficulties of coupling piezoelectric transducers with curved surfaces. To date, the authors [1] have been interested in acoustic generation for opaque cylinders where the acoustic source is located at the cylinder surface.

In this work, assuming line focusing of the laser pulses, we propose a two-dimensional (2D) semi-analytical model for acoustic waves generation and propagation in a partly transparent isotropic cylinder. First, the radial displacement at any position on the free surface is derived, in a 2D Fourier domain, for an inner point source. The response to a volume-source distribution along a radius is obtained as a convolution of the above Green function with the corresponding source distribution caused by optical absorption. Two inverse transforms are then applied to obtain the radial displacement at the cylinder surface.

Second, picosecond ultrasonics experiments are performed on a tungsten micrometric fiber of 5 μm diameter and compared with calculated waveforms.

2 Photoelastic generation in fibers

Let us consider a homogenous and isotropic cylinder of infinite length, radius a , and density ρ . Line focusing of a laser pulse at the cylinder surface along its z -axis is assumed. The thermoelastic fields due to the laser line pulse along the z -axis direction are governed by the following coupled equations of thermoelasticity

$$\begin{aligned} \nabla \cdot (\bar{\kappa} : \nabla T) + T_0 \beta \nabla \cdot \frac{\partial \mathbf{u}}{\partial t} - Q &= \rho C_p \frac{\partial T}{\partial t}, \\ (\lambda + 2\mu) \nabla \nabla \cdot \mathbf{u} - \mu \nabla \times \nabla \times \mathbf{u} &= \rho \frac{\partial^2 \mathbf{u}}{\partial t^2} + \tilde{\beta} \nabla T \end{aligned} \quad (1)$$

where $\bar{\kappa}$ is the thermal conductivity tensor of the second order, T_0 the room temperature expressed in Kelvin, $\beta = 3\lambda + 2\mu$ the thermal modulus with λ and μ the Lamé coefficients and C_p the specific heat. The source term Q in the heat equation (1.1) is due to the laser optical pulse and corresponds to an opto-thermal energy conversion and is expressed in unit of a volume density power ($[Wm^{-3}]$). The second equation (1.2) stands for the well known equilibrium law where \mathbf{u} is the displacement vector and $\tilde{\beta} = \beta/(\lambda + 2\mu)$.

Thermal source $Q(r, \theta, t)$ expresses a volume distribution of optical sources in the cylinder due to optical absorption over a characteristic length α^{-1} , where α is the extinction coefficient. According to the symmetry of the problem, absorption phenomena lies essentially in the radial direction whereas orthoradial dependance is only due to the width of the line source included

in the model by mean of the gaussian shape function $g(\theta) = 1/(2a\gamma\sqrt{\pi})e^{-\theta^2/4\gamma^2}$ [m^{-1}] where γ is the angle corresponding to the linewidth. So, the thermal source Q can be written in the following form,

$$\begin{aligned} Q(r, \theta, t) &= \alpha E g(\theta) \delta(t) \mathcal{D}(r), \\ \text{where } \mathcal{D}(r) &= \begin{cases} e^{-\alpha(a-r)}, & \theta = 0 \\ e^{-\alpha(a+r)}, & \theta = \pi \end{cases} \end{aligned} \quad (2)$$

The incoming lineic laser energy E_0 ($[Jm^{-1}]$) is partially reflected at the surface of the sample with the reflection coefficient R . Thus, the transmitted energy is given by $E = E_0(1 - R)$.

We assume that the evolution of the temperature field doesn't depend on the mechanical field \mathbf{u} and so the coupling term can be neglected in equation (1.1) leading to a partly coupled thermoelasticity problem. In this work, we are mainly interested in very few thermal diffusive materials and so we neglect heat conduction. First, solving (1.1) we derive the temperature elevation field ΔT

$$\Delta T(r, \theta, t) = \frac{\alpha E}{\rho C_p} g(\theta) H(t) \mathcal{D}(r) \quad (3)$$

We find out a temperature elevation field ΔT with a Heaviside time dependance $H(t)$ satisfying the assumption of no heat conduction. Then, thermal field being obtained we can solve the uncoupled mechanical problem,

$$\begin{aligned} \nabla^2 \varphi - \frac{1}{c_L^2} \frac{\partial^2 \varphi}{\partial t^2} &= \tilde{\beta} \Delta T, \\ \nabla^2 \psi - \frac{1}{c_T^2} \frac{\partial^2 \psi}{\partial t^2} &= 0 \end{aligned} \quad (4)$$

where φ and Ψ are scalar and vector potentials respectively and $c_L = \sqrt{\frac{\rho}{\lambda + 2\mu}}$, $c_T = \sqrt{\frac{\rho}{2\mu}}$ are the longitudinal respectively shear wave velocities. Free boundary condition is considered,

$$\begin{aligned} \sigma_{rr}(r = a) &= 0, \\ \sigma_{r\theta}(r = a) &= 0 \end{aligned} \quad (5)$$

3 Transformed displacement solution in term of potential Green function

In order to derive a solution to the above boundary value problem, let us derive the Green function $G(r|r_0)$, expressed in a potential form, for the interior problem of a dilatational line source located at the position ($r_0 < a, \theta_0 = 0$) inside the cylinder.

$$\begin{aligned} \nabla^2 g(r|r_0) + p^2 g(r|r_0) &= \tilde{\beta} \frac{\delta(r-r_0)}{r_0}, \\ \nabla^2 \psi(r|r_0) + s^2 \psi(r|r_0) &= 0 \end{aligned} \quad (6)$$

with $p = \omega/c_L$ and $s = \omega/c_T$. Then the so-called Green function is explicitly given by

$$\mathbf{G}(r|r_0) = \nabla g(r|r_0) + \nabla \times \boldsymbol{\psi}(r|r_0) \quad (7)$$

Where $g(r|r_0)$ and $\boldsymbol{\psi}(r|r_0)$ are respectively solution of (6.1) and (6.2).

Solution for (6.1) may be sought as a linear combination of the two independent solutions of the homogeneous Helmholtz equation[2]

$$g(r|r_0) = A_\nu J_\nu(pr) H(r_0 - r) + [B_\nu Y_\nu(pr) + C_\nu J_\nu(pr)] H(r - r_0), \quad r_0 < a \quad (8)$$

where $H(r)$ corresponds to a radial Heaviside distribution. Solution of (6.2) gives us another unknown constant D_ν to find out,

$$\boldsymbol{\psi}(r|r_0) = D_\nu J_\nu(sr) \quad (9)$$

Four constants have to be found out injecting expressions of $g(r|r_0)$ and $\boldsymbol{\psi}(r|r_0)$ into the two equations of boundary condition. Consideration on continuity properties between the left hand side of equation (6.1) and the δ -function in the right hand side gives us two additional equations which permit to determinate the two others constants. Solving the corresponding linear system of equations allows us to derive the Green function for the radial displacement at a given position at the surface of the cylinder due to a dilatational line source located into the cylinder with the corresponding free boundary conditions.

$$G_r^v(a|r_0, \nu, \omega) = \frac{\pi \tilde{\beta}}{2a} J_\nu(pr_0) \left[Y_\nu(pa) \left(\mathcal{Y}_a - \frac{E_\nu}{D_\nu} \mathcal{P}_a \right) + \frac{2\nu^2}{\pi D_\nu} \left(1 - \nu^2 + \frac{s^2 a^2}{2} \right) \right] \quad (10)$$

with $\mathcal{Y}_a = paY'(pa)/Y(pa)$, $\mathcal{P}_a = paJ'(pa)/J(pa)$, $\mathcal{S}_a = saJ'(sa)/J(sa)$, and where $D_\nu(\nu, \omega) = 0$ corresponds to the dispersion equation, and

$$E_\nu = \left(\nu^2 - \frac{s^2 a^2}{2} \right)^2 - \nu^2 + \frac{s^2 a^2}{2} (\mathcal{P}_a + \mathcal{Y}_a) + (1 - \nu^2) \mathcal{P}_a \mathcal{Y}_a \quad (11)$$

The radial displacement field is then theoretically derived thanks to a convolution between the radial component of the Green function $G_r^v(a|r_0)$, due to an inside dilatational line source, and the radial distribution of acoustic sources which is in our case related to the thermal field.

$$U_r(a, \nu, \omega) = \int_0^{a^-} G_r^v(a|r_0, \nu, \omega) T(r_0, \nu, \omega) r_0 dr_0 \quad (12)$$

Finally, radial displacement in the real space is obtained using 2D inverse Fourier Transform. In order to avoid difficulties in numerical integration due to poles of the dispersion equation $D_\nu(\nu, \omega) = 0$, Weaver[3] proposed to introduce a small imaginary part in the frequency variable $\omega^* = \omega - j\delta$ to move the poles out of the real axis.

$$U_r(a, \theta, t) = \frac{e^{\delta t}}{2\pi} \int_{-\infty}^{\infty} \sum_{\nu=-\infty}^{\infty} U_r(a, \nu, \omega) e^{j(\nu\theta - \omega t)} d\omega$$

Noting that $U_r(r, \nu, \omega)$ is an even function for the ν variable, radial displacement can be rewritten as following,

$$U_r(a, \theta, t) = \frac{e^{\delta t}}{\pi} \int_{-\infty}^{\infty} \left\{ \sum_{\nu=0}^{\infty} U_r(a, \nu, \omega) \cos(\nu\theta) \right\} e^{-j\omega t} d\omega$$

4 Numerical and Experimental validation

Picosecond ultrasonics setup (Fig.1) is used to perform experiments on a tungsten micrometric fiber with a diameter of 5 μm . Generation and detection points are spatially superposed and shifted in time thanks to a delay line providing a time resolved technique[4]. Tungsten fiber is stretched at its bounds and is totally free of contact over a distance of one millimeter in order to prevent any perturbation of the cylindrical surface waves. Beam distortion detection (bdd) technique[5] is applied

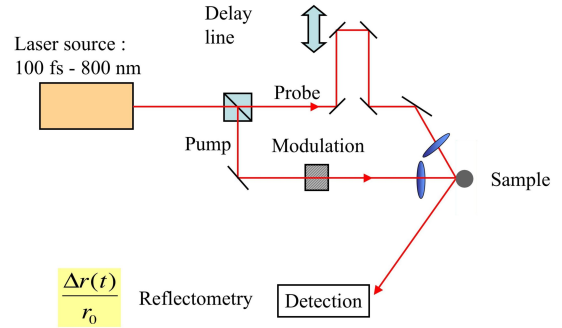


Figure 1: Picosecond ultrasonics setup.

to measure reflectivity changes in the sample. This measured quantity is composed of an interferometric component, and of two reflectometric components with and without diaphragm on the probe beam path.

$$\frac{\Delta R}{R_0} = j \frac{\Delta R_i}{R_0} + \frac{\Delta R_r}{R_0} + \frac{\Delta R_d}{R_0} \quad (13)$$

In the remainder of the paper, we focus on the reflectometric part of the signal (i.e. real part of equation (13)) because interferometric component $j \frac{\Delta R_i}{R_0}$ is not measured. Whereas $\Delta R_r/R_0$ is related to strain, Chigarev[5] has shown that $\Delta R_d/R_0$ can be estimated as a term proportional to the displacement of the surface of the sample when a small diaphragm aperture is used. For tungsten, acoustic wavelength is about $\Lambda \approx 50$ nm which is the same order as the light penetration $\xi \approx 20$ nm and in this case we obtain $\Delta R_d/\Delta R_r \approx 1$ [5]. Thus, the measured signal is a mixture of the strain and displacement signals.

The wavelength of the pump beam is 400 nm whereas that of the probe one is 800 nm, and the auto-correlation width of the two beams is measured as 1 μm . Experimental result is compared to a numerical simulation obtained with the two-dimensional photoelastic model for fibers for a source width of 0.5 μm . Imaginary part of the frequency, used to remove poles from the real axis, is

introduced with the numerical parameter $\delta = 0.02$. Material constants used for simulation are $c_{11} = 522$ GPa, $c_{12} = 200$ GPa, $\rho = 19.3$ g.cm $^{-3}$, a small imaginary part is introduced in the stiffness coefficients $c_{ij}^* = c_{ij} + j\omega\eta$ with $\eta = 0.05$ GPa.s $^{-1}$ to take into account attenuation of acoustical waves. Reflexion coefficient for tungsten is chosen to be $R = 0.5$.

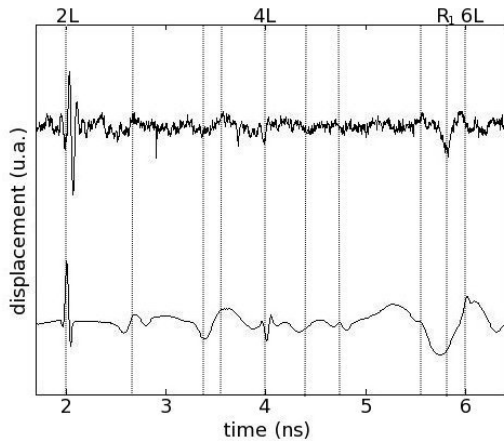


Figure 2: Comparison between bdd experiment signal (top) and theoretical displacement (bottom) on tungsten fiber of 5 μm diameter. Thermal background was removed from the experimental data.

A quite good agreement is obtained (Fig.2) in term of time arrivals for the longitudinal waves $2L$, $4L$ propagating back-and-forth through the fiber. Strong attenuation is observed for the $4L$ echo which has travelled about 20 μm and encountered up to three successive reflexions. As expected Rayleigh wave R_1 is clearly detected with a spread shape echo.

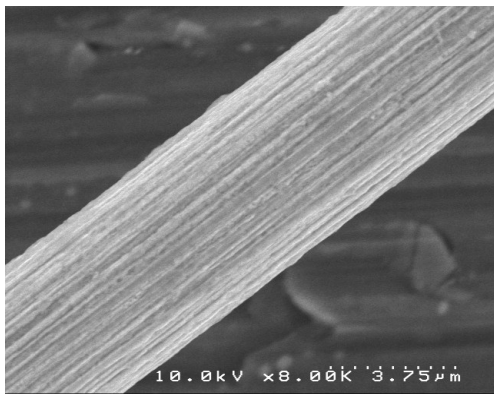


Figure 3: Photograph of a tungsten micrometric fiber captured from Scanning Electron Microscopy.

This comparison is a very first step in the understanding of acoustic waves propagation in such micrometric fiber. The mixture between strain and displacement in the measured signal doesn't allow to clearly compare the shape of the echoes but only their time arrivals. Numerical simulation permits us to identify main arrivals as longitudinal reflexions $2L$, $4L$ and Rayleigh wave R_1 . However, even if other peaks are not clearly identified we can expect that some correspond to transverse or waves resulting of mode conversion. Then, it would be possible to obtain information on the stiffness

coefficient c_{12} . One limitation concerns the building process of this kind of metallic fibers which implies a quite bad surface quality of the fiber explaining the bad Signal to Noise Ratio. Scanning Electron Microscopy technique allows to access an image (Fig.3) of the fiber surface and confirms the bad surface quality of this sample.

5 Conclusion

Time resolved picosecond ultrasonics technique is especially suited for the study of acoustical physics in micrometric or sub-micrometric structures. At these low scales, photo-thermal mechanisms have to be considered for the waves generation process taking into account the light penetration depth in the sample. We propose a two-dimensionnal photo-elastic model for generation and propagation of acoustical waves in cylindrical structures based on a radial displacement Green function. Convolution theorem is then applied to obtain the response to a radial distribution of acoustic sources. Theoretical results are compared to a picosecond ultrasonics experiment on a tungsten micrometric fiber with a diameter of 5 μm . Good agreement is obtained in term of time arrivals and main echoes were identified like the diametrically sequences of longitudinal waves $2L$, $4L$, and the cylindrical Rayleigh wave R_1 . However, further study has to be achieved to identify other interesting peaks that could represent transverse or waves resulting of mode conversion useful to perform the inverse problem for such micrometric fiber.

References

- [1] Y. Pan, C. Rossignol, B. Audoin, "Acoustic waves generated by a laser line pulse in a transversely isotropic cylinder", *Applied Physics Letters* 82, 4379-4381 (2003)
- [2] G.N. Watson, "A treatise on the theory of Bessel fonctions", *Cambridge University Press*, (1966)
- [3] R. Weaver, W. Sachse, K. Kim, "Transient elastic waves in a transversely isotropic plate", *J. Appl. Mech.* 63, 338-346 (1996)
- [4] C. Thomsen, J. Strait, Z. Vardeny, H.J. Maris, J. Tauc, J.J. Hauser, "Coherent phonon generation and detection by picosecond light pulses", *Phys. Rev. Lett.* 53(10), 989 (1984)
- [5] N.V. Chigarev, C. Rossignol, B. Audoin, "Surface displacement measured by beam distortion detection technique : application to picosecond ultrasonics", *Rev. Sci. Instrum.* 77(11), 114901 (2006).